

*Citation for published version:*

Walsh, A 2015, 'Principles of Chemical Bonding and Band Gap Engineering in Hybrid Organic–Inorganic Halide Perovskites', *Journal of Physical Chemistry C*, vol. 119, no. 11, pp. 57555760. <https://doi.org/10.1021/jp512420b>

*DOI:*

[10.1021/jp512420b](https://doi.org/10.1021/jp512420b)

*Publication date:*

2015

*Document Version*

Publisher's PDF, also known as Version of record

[Link to publication](#)

*Publisher Rights*

CC BY

**University of Bath**

**Alternative formats**

If you require this document in an alternative format, please contact:  
[openaccess@bath.ac.uk](mailto:openaccess@bath.ac.uk)

**General rights**

Copyright and moral rights for the publications made accessible in the public portal are retained by the authors and/or other copyright owners and it is a condition of accessing publications that users recognise and abide by the legal requirements associated with these rights.

**Take down policy**

If you believe that this document breaches copyright please contact us providing details, and we will remove access to the work immediately and investigate your claim.

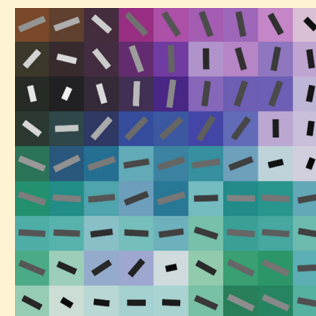


# Principles of Chemical Bonding and Band Gap Engineering in Hybrid Organic–Inorganic Halide Perovskites

Aron Walsh\*

Centre for Sustainable Chemical Technologies and Department of Chemistry, University of Bath, Claverton Down, Bath BA2 7AY, U.K.

**ABSTRACT:** The performance of solar cells based on hybrid halide perovskites has seen an unparalleled rate of progress, while our understanding of the underlying physical chemistry of these materials trails behind. Superficially,  $\text{CH}_3\text{NH}_3\text{PbI}_3$  is similar to other thin-film photovoltaic materials: a semiconductor with an optical band gap in the optimal region of the electromagnetic spectrum. Microscopically, the material is more unconventional. Progress in our understanding of the local and long-range chemical bonding of hybrid perovskites is discussed here, drawing from a series of computational studies involving electronic structure, molecular dynamics, and Monte Carlo simulation techniques. The orientational freedom of the dipolar methylammonium ion gives rise to temperature-dependent dielectric screening and the possibility for the formation of polar (ferroelectric) domains. The ability to independently substitute on the A, B, and X lattice sites provides the means to tune the optoelectronic properties. Finally, ten critical challenges and opportunities for physical chemists are highlighted.



## ■ INTRODUCTION

Hybrid organic–inorganic halides have been of interest since the start of the 20th century;<sup>1</sup> however, the first report of a perovskite-structured hybrid halide appears to have been by D. Weber in 1978.<sup>2,3</sup> In the same journal volume, he reported both  $\text{CH}_3\text{NH}_3\text{PbX}_3$  ( $\text{X} = \text{Cl}, \text{Br}, \text{I}$ ) and the  $\text{CH}_3\text{NH}_3\text{SnBr}_{1-x}\text{I}_x$  solid solution. In the subsequent decades, these materials were studied in the context of their solid-state chemistry and physics,<sup>4–6</sup> with the first solar cell reported in 2009.<sup>7</sup> The resulting explosion of research effort and success in the photovoltaic applications of these materials has been the subject of many review papers and commentaries.<sup>8–14</sup>

Hundreds of materials have been tried and tested for use as light absorbing layers in solar cells, so one question has been frequently posed: *what makes hybrid halide perovskites special?* The question is difficult to answer with certainty as our understanding of the physical properties of these materials, including how the solar cells operate, continues to evolve. One of the unique features of this class of material is their large dielectric constants ( $\epsilon_0 > 20$ ), compared to conventional semiconductors ( $\epsilon_0 < 20$ ), which include a rotational component associated with molecular dipole relaxation.

The aim of this Feature Article is to step back and recount the fundamental physical chemistry underpinning the performance—and potential limitations—of hybrid perovskite materials. The work discussed here is primarily from our research group;<sup>13,15–21</sup> however, many others have contributed to the computational studies in the area. Simulations on the electronic structure, alloy formation, and lattice defects have been the subject of recent review papers.<sup>22–25</sup>

We previously produced a gentle introduction to the fundamental chemistry of hybrid perovskites,<sup>17</sup> which is not duplicated here. Instead, we first discuss the principles of

chemical bonding in these systems, followed by approaches to tune the electronic structure, and finally outline ten outstanding challenges in the field.

## ■ CHEMICAL BONDING

The chemical bonding in hybrid perovskites with  $\text{ABX}_3$  stoichiometry (shown in Figure 1) can be separated into three distinct components. It should be noted that these materials are organic–inorganic but *not* organometallic—following the IUPAC definition—as there is no direct bond between a metal and carbon atom. In the context of metal–organic frameworks, they are considered to be  $\text{I}^3\text{O}^0$  materials<sup>29</sup> due to the combination of a three-dimensional inorganic network with a zero-dimensional (molecular) organic component.

**a. Metal Halide Framework.** The bonding within the  $\text{BX}_3^-$  anionic framework is unambiguously heteropolar (mixed ionic/covalent interactions). The formal oxidation states of  $\text{Pb}(+2)$  and  $\text{I}(-1)$ , resulting from the chemical composition, are a good approximation of the chemical species here. Electrostatic interactions dominate between ions with net charge. As usual, the quantification of partial charges remains ill-defined due to the collective nature of the periodic electronic wave function.<sup>30,31</sup> The Born effective charges in halide perovskites are large (the value for Pb can exceed 4),<sup>32</sup> consistent with high ionicity.

The lattice energy (defined with respect to the ions held infinitely far apart) and electrostatic site potentials are listed for

**Received:** December 13, 2014

**Revised:** January 22, 2015

**Published:** February 6, 2015



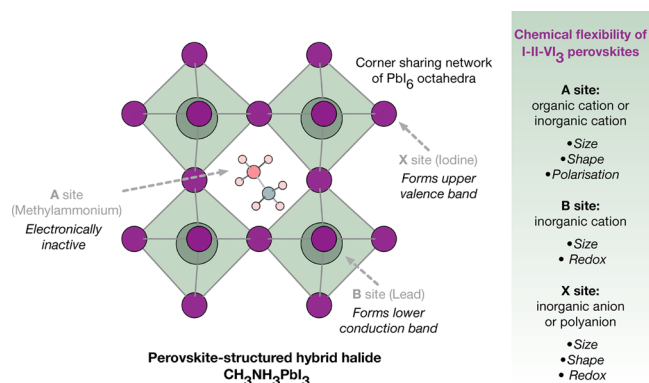


**Figure 1.** Schematic of the perovskite crystal structure with respect to the A, B, and X lattice sites. The redox chemistry of the component ions can be used to influence the valence and conduction band energies and orbital composition, and hence the stability of electrons and holes in the material.<sup>26</sup> Note that for larger molecular A sites layered perovskites are formed.<sup>27,28</sup> Beyond halide perovskites, a wider range of stoichiometries and superstructures are known, e.g., the Ruddlesden–Popper, Aurivillius, and Dion–Jacobson phases.

**Table 1.** Lattice Energy (eV/cell) and Site Madelung Potentials (in units of V) for a Range of ABX<sub>3</sub> Perovskite Compositions (Cubic Lattice,  $a = 6 \text{ \AA}$ ) Assuming the Formal Oxidation State of Each Species<sup>a</sup>

stoichiometry	$E_{\text{lattice}}$	$V_{\text{A}}$ (V)	$V_{\text{B}}$ (V)	$V_{\text{X}}$ (V)
I–V–VI <sub>3</sub>	–140.48	–8.04	–34.59	16.66
II–IV–VI <sub>3</sub>	–118.82	–12.93	–29.71	15.49
III–III–VI <sub>3</sub>	–106.92	–17.81	–24.82	14.33
I–II–VII <sub>3</sub>	–29.71	–6.46	–14.85	7.75

<sup>a</sup>The potentials are aligned to a common vacuum level at 0 V. The hybrid halide perovskites are of type I–II–VII<sub>3</sub>. Reprinted with permission from ref 17. Copyright 2014 American Chemical Society.

a range of perovskite stoichiometries in Table 1. In comparison to the three types of oxide (group VI anion) perovskite, for the halide (group VII anion) perovskite the electrostatic stabilization is notably reduced. The lattice energy is just  $-29.71 \text{ eV}$  per ABX<sub>3</sub> cell, with an electrostatic potential on the anion site ca. 50% of the group VI anions. Due to this weaker potential alone, lower ionization potentials (workfunctions) are expected for halide perovskites compared to, for example, metal oxides.<sup>33,34</sup> A second consequence is that lattice vacancies are facile to form<sup>21</sup> and do not result in deep ionization levels. In contrast, for rocksalt-structured metal halides, the halide is in an octahedral coordination environment with a large confining electrostatic potential. In such cases, a halide vacancy will trap electrons with ionization levels deep in the band gap: an F-center.

For  $\text{CH}_3\text{NH}_3\text{PbI}_3$ , the formal electronic configurations of Pb  $6s^26p^0$  and I  $5p^6$  are apparent from the electronic band structure, where the upper valence band is formed from the I p orbitals and the lower conduction band is formed from the unoccupied Pb p orbitals. There is an admixture of Pb s in the valence band, but here the cationic lone pair electrons are stereochemically inactive,<sup>35</sup> at least in the equilibrium structural configuration. Polar instabilities of the Pb(II) ion are common in ferroelectric and multiferroic oxide perovskites.<sup>36</sup>

Strong hybridization (orbital overlap) along the octahedral framework results in light electron ( $0.15 m_e$ ) and hole ( $0.12 m_e$ ) effective masses a fraction of the free electron mass.<sup>19</sup> These light carrier masses provide the means for high-mobility band transport in high-quality materials. The high atomic numbers of lead and iodine suggest that relativistic effects are important for an accurate determination of the electronic structure.<sup>19</sup> Many-body electron–electron interactions have been shown to be important. These factors combine to make high-quality electronic structure studies, such as relativistic GW theory, computationally and methodologically challenging. While density functional theory calculations can now be performed routinely on system sizes of up to 100 s of atoms,

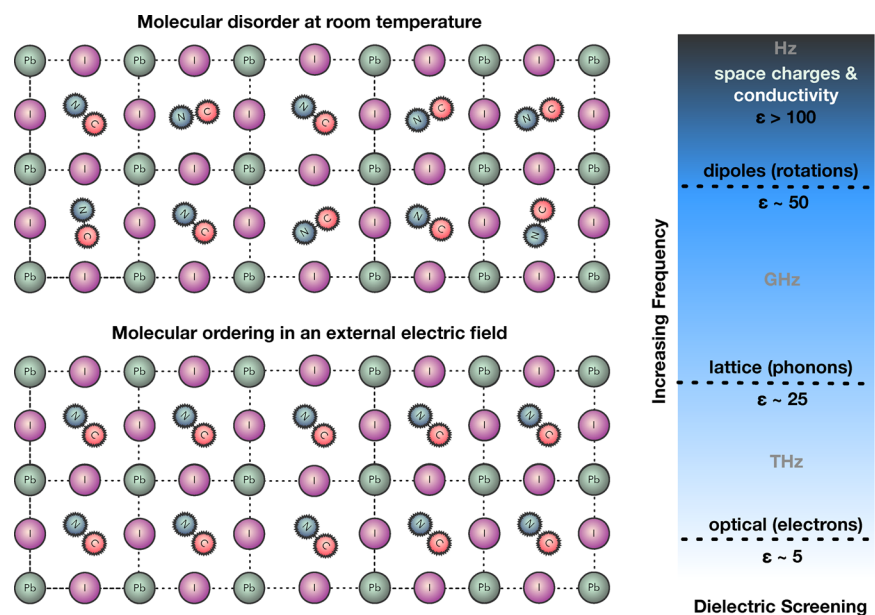


**Figure 2.** Schematic of the ordering of molecular dipoles in the presence of an external electric field, as well as the four regimes in the dielectric response from lowest frequency (electronic excitations) to highest frequency (space charges and electronic or ionic conductivity). Each process will have a characteristic relaxation time and can combine to give a complex temporal response to an external perturbation.

for relativistic quasi-particle self-consistent GW theory  $\text{CH}_3\text{NH}_3\text{PbI}_3$  represents the most complex system studied to date. Note that this approach is superior to non-self-consistent  $G_0W_0$  methods but still neglects electron–phonon coupling, which may be important for these structurally soft materials.

**b. Intermolecular Interaction.** Methylammonium is a closed-shell 18-electron cation. (In contrast to several erroneous statements in the published literature,  $\text{CH}_3\text{NH}_3^+$  is not a free radical.) The  $\text{CH}_3\text{NH}_3^+$  molecules in neighboring cages are  $\sim 6$  Å apart. The large permanent electric dipole (2.29 D with respect to the center of charge of the ion) results in an estimated electrostatic point dipole–dipole interaction energy of 25 meV.<sup>16</sup> For two static dipoles, the interaction tails off as  $(1/r^3)$ ; however, the screening effect of two freely rotating dipoles shortens this Keesom force (one component of the van der Waals interaction) to  $(1/r^6)$ .

As the dipole–dipole interaction energy is comparable to available thermal energy at room temperature, we expect a complex ferroelectric behavior. Monte Carlo simulations have shown that for a fixed lattice a striped antiferroelectric alignment of dipoles is favored at low temperatures, which become increasingly disordered and finally paraelectric at high temperatures.<sup>17</sup> At room temperature, there is significant local structure which can be linked with regions of high and low electrostatic potential. Even for a single-crystal film the topology of the electrostatic potential resembles a bulk heterojunction more familiar to organic photovoltaics. Larger polar domain structures have recently been observed from piezoelectric force microscopy, which may be associated with effects from local chemical and lattice strain.<sup>37</sup> Tunable ferroelectric polarization has also been predicted to occur in the Sn analogues.<sup>38</sup>

The orientation of molecular dipoles is involved in the unusual dielectric response of  $\text{CH}_3\text{NH}_3\text{PbI}_3$ . At high (optical) frequencies, there exists the standard *electronic* response of the system to an applied electric field. At lower (THz) frequencies, an additional *vibrational* response from lattice phonons gives rise to the static dielectric constant of 25 (previously computed from density functional perturbation theory).<sup>19</sup> The molecular response occurs at even lower frequencies (GHz regime), which can be associated with *rotational* order. Toward audio frequencies a “colossal” permittivity emerges, which can be linked to ionic and/or electronic conductivity: the Maxwell–Wagner effect. These contributing factors are summarized in Figure 2.

**c.. Molecule–Framework Interaction.** The dominant bonding between the molecule (A site) and framework is electrostatic in nature.  $\text{CH}_3\text{NH}_3^+$  is a positively charged ion inside a negatively charged cage, so there is a strong electrostatic potential ( $\sim 8$  V; Table 1) holding the molecule at its lattice site.

An additional electrostatic contribution to the chemical bonding between the molecular dipole and the  $\text{PbI}_6$  octahedra is the charge–dipole interaction, which is dependent on the dipole orientation. There is also the effect of primary polarization. Given the appreciable polarizability of the  $\text{I}^-$  ions (ca.  $7 \times 10^{-24}$  cm<sup>3</sup>), an induced dipole interaction is expected (the so-called Debye force). Due to these interactions, a correlation is expected between molecular orientation and octahedral deformation in molecular dynamic simulations;<sup>17</sup> more in-depth studies are ongoing. The molecular dipole–framework interaction has also been discussed in terms of hydrogen bonds; however, both interactions are electrostatic in

nature and are difficult to distinguish between. The significant mobility of the cations (including hydrogen atoms) at room temperature<sup>16</sup> does suggest that a dipole interaction is a more appropriate and general description.

The van der Waals interaction collectively describes the intermolecular (Keesom force) and molecule–framework (Debye force) interactions discussed above. It should be noted, however, that the term “van der Waals” is sometimes used synonymously with “London dispersion”. Within density functional theory, there are now many flavors of dispersion-corrected exchange–correlation functional, which aim to recover a description of the London force (secondary polarization) associated with dynamic correlation. By taking a first-generation generalized-gradient functional (e.g., PBE<sup>39</sup>) which overestimates equilibrium bond lengths by 1–2%, the addition of a weakly attractive  $r^{-6}$  potential will result in better agreement with experimental structures. It does not require that these interactions are “London dispersion” in nature. Our approach has been to employ a functional optimized for solids (e.g., PBEsol<sup>40</sup> or HSE06<sup>41</sup>), which quantitatively describes structural parameters of dense materials without system-specific parametrization. In addition to improved lattice parameters, PBEsol also describes the vibrational properties of solid-state systems more accurately.<sup>42</sup>

From this discussion, it is clear that a variety of interactions give rise to the properties of the hybrid perovskites important to their photovoltaic performance. In particular, the combination of the light carrier effective masses provided by the metal halide framework and the strong dielectric screening—including the molecule–framework and intermolecular interactions—favors free carrier generation over excitons (bound electron–hole pairs) upon illumination.

## BAND GAP ENGINEERING

It is possible to chemically substitute on all of the perovskite lattice sites, and appropriate examples of each can be found in the literature. It is important to recognize the chemical distinction between the three approaches.

In the limit of a small perturbation, the physical response to a hydrostatic volume change can be described by the band gap deformation potential<sup>43</sup>

$$\alpha_V = \frac{\partial E_g}{\partial \ln V} \quad (1)$$

which for  $\text{CH}_3\text{NH}_3\text{PbI}_3$  is positive ( $\alpha_V^R = 2.45$  eV).<sup>17</sup> As the fundamental band gap is determined at the boundary of the Brillouin zone ( $R$  for the pseudocubic structure), the out-of-phase band-edge states are stabilized as the lattice expands. Temperature-dependent photoluminescence indicates a decrease in band gap with decreasing temperature (lattice contraction) from 1.61 eV at 300 K to 1.55 eV at 150 K, which is at the onset of a phase change.<sup>44</sup> The chemical effects of substitution will generally exceed this physical volume effect, as discussed below.

**A-Site Substitution.** The A site of  $\text{CH}_3\text{NH}_3\text{PbI}_3$  does not directly contribute to the frontier electronic structure, but it can have an *indirect* influence by changing the crystal structure (Figure 3).

Following eq 1, lower band gap values should be observed for smaller molecular cations. The replacement of  $\text{CH}_3\text{NH}_3^+$  by  $\text{NH}_4^+$  in the perovskite lattice reduces the band gap by 0.3 eV.<sup>19</sup> The smallest possible counterion is a proton ( $\text{H}^+$ );  $\text{HPbI}_3$  has a



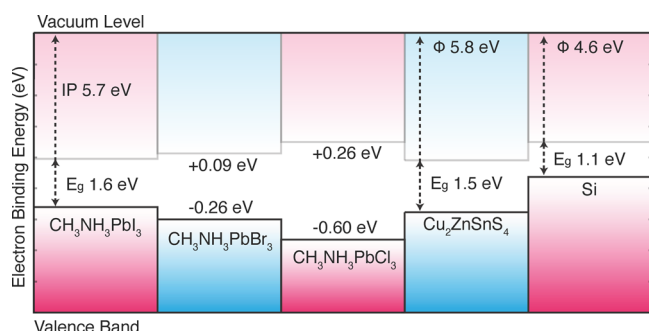


**Figure 3.** Calculated natural band offsets of  $\text{CH}_3\text{NH}_3\text{PbI}_3$  and related materials based on density functional calculations (with quasi-particle corrections). Interfacial or surface electric dipoles (or quadrupoles) are not considered here. Adapted with permission from ref 17. Copyright 2014 American Chemical Society.

theoretical cubic perovskite lattice parameter of 6.05 Å and an associated band gap of less than 0.3 eV.<sup>17</sup>

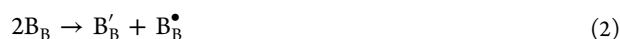
The limitation of this logic (hydrostatic deformation) is the relationship between the size of the ion and the local structure. For example, in reality both  $\text{NH}_4\text{PbI}_3$  and  $\text{HPbI}_3$  adopt alternative chain or layer structures due to a mismatch in ionic radius.<sup>45,46</sup> The geometric constraints for the formation of a stable perovskite lattice are summed up in the radius ratio rules, which have been recently extended to hybrid perovskites.<sup>47</sup> An A-site ion too small for the  $\text{BX}_3$  framework results in an instability of the octahedral networks with respect to tilting, which can change the electronic properties (e.g., a transition from an antiferroelectric to ferroelectric phase).

$\text{CH}_3\text{NH}_3\text{PbI}_3$  has a Goldschmidt tolerance factor of 0.91 (unstable with respect to tilting).  $\text{NH}_4\text{PbI}_3$  has a tolerance factor of 0.76, and an alternative nonperovskite structure is favored. More asymmetric molecular ions (e.g., formamidinium,  $\text{NH}_2\text{CHNH}_2^+$  or FA) can also result in “built-in” structural distortions due to their deviation from spherical symmetry. The chemical and physical strains associated with the molecular substitution cannot be neglected when considering band gap engineering.<sup>48</sup>

The choice of A-site ions that are too large for the  $\text{BX}_3$  framework can result in layered perovskite structures (e.g., Ruddlesden–Popper type  $\text{A}_{n-1}\text{A}'_2\text{B}_n\text{X}_{3n+1}$  phases). The quantum confinement associated with these layered structures has itself attracted significant interest.<sup>27,28</sup>

**B-Site Substitution.** Substitution on the B site can be used to directly alter the conduction band. Isovalent substitution of Pb for Sn has been successfully reported;<sup>49</sup> however, Sn(II) is less chemically stable in an octahedral environment.<sup>50</sup> Oxidation to Sn(IV) results in the low performance and high carrier concentrations found for the Sn halide perovskites. The stability of Ge(II) is further reduced, owing to its lower binding energy 4s<sup>2</sup> electrons and is unlikely to result in a candidate photovoltaic material.

The so-called “double” perovskites are well-known for metal oxides. Here the B site is substituted by two aliovalent ions (one higher and one lower oxidation state)



An example here would be the substitution of Pb(II) by Bi(III) and Tl(I), which is likely to reduce the electronic band gap due to the lower binding energy of the Bi 6p orbitals and the fluctuations in electrostatic potential caused by the combination

of monovalent and trivalent ions. An advantage of this approach is that controlled substitutions beyond the 1:1 stoichiometry could be used to influence the n-type (excess Bi) or p-type (excess Tl) carrier concentrations.

**X-Site Substitution.** For  $\text{CH}_3\text{NH}_3\text{PbI}_3$ , the anion (X site) dictates the valence band energy.<sup>15</sup> The observed band gap changes upon halide substitution are influenced by the electronic states of the anion; i.e., from Cl to Br to I the valence band composition changes from 3p to 4p to 5p with a monotonic decrease in electron binding energy (lower ionization potential). The valence band energy varies by as much as 0.6 eV between the methylammonium chloride and iodide perovskites. This holds true for other choices of the molecular ion: the substitution of Br by I in  $\text{FAPbX}_3$  decreases the optical band gap from 2.23 to 1.48 eV.<sup>51</sup>

The successful incorporation of the tetrafluoroborate polyanion into the perovskite structure has been recently reported.<sup>52</sup> We have shown, however, that both  $\text{BF}_4^-$  and  $\text{PF}_6^-$  do not hybridize significantly with Pb, which results in an increase in the band gaps and a decrease in the band widths.<sup>20</sup> Such substitutions, if stable structures were formed, could be exploited to produce a novel high-*k* dielectric with potential applications in transistors or memristors.

## CONCLUSION AND CHALLENGES

In addition to their application in photovoltaics, hybrid halide perovskites display a rich physical chemistry. We have discussed the salient features of their chemical bonding and routes to tuning the properties beyond the widely studied methylammonium lead iodide.

Hybrid halide perovskites still pose many fundamental challenges relating to their physical chemistry and chemical physics. Ten issues of current interest include:

1. Local structure — the average crystal structure inferred from standard X-ray diffraction experiments is likely to be far from the local structure of the perovskite framework.
2. Dynamic disorder — knowledge is required of the time scales associated with molecular motion and how this changes from single crystals to thin films and with the method of preparation.
3. Lattice point defects — there have been reports of n-type, p-type, and intrinsic semiconducting samples of  $\text{CH}_3\text{NH}_3\text{PbI}_3$ . What causes this behavior, and how can the semiconductivity be controlled?
4. Ionic conductivity — many perovskite materials support vacancy-mediated ion diffusion. Is iodine, methylammonium, or hydrogen mass transport contributing to low-frequency impedance spectra?
5. Surface and interfaces — the chemical nature of extended defects is poorly understood, in particular the interface between the perovskite and the hole transport layer.
6. Ferroelectricity — simulations demonstrate short-range ferroelectric order at room temperature; however, external electric fields and internal strains will change this behavior.
7. Grain boundaries and domain walls — the perovskite microstructure may provide alternative pathways for conductivity and electron–hole separation or recombination. What is their form and abundance?

8. Increased stability — the long-term air instability of these materials is in part associated with the volatility of the molecular components. The development of alternative ions without labile protons would be advantageous.
9. Pb-free compositions — a major goal remains to identify a (stable) Pb-free material that maintains the same exceptional performance as  $\text{CH}_3\text{NH}_3\text{PbI}_3$  in solar cells. The difficulty is in maintaining a small band gap with lighter metals.
10. Device models — there are standard electron transport models for p–n junction devices and extensions to bulk heterojunctions; however, there is no band transport model that encompasses the complex behavior of the hybrid perovskites including current–voltage hysteresis.

## AUTHOR INFORMATION

### Corresponding Author

\*E-mail: a.walsh@bath.ac.uk; Twitter: @lonepair.

### Notes

The authors declare no competing financial interest.

### Biography



**Prof. Aron Walsh** holds the Chair of Materials Theory in the Centre for Sustainable Chemical Technologies at the University of Bath. He was awarded his BA and Ph.D from Trinity College Dublin (Ireland), completed a postdoctoral position at the National Renewable Energy Laboratory (USA), and held a Marie Curie fellowship at University College London (UK). His research combines computational technique development and applications at the interface of solid-state chemistry and physics.

## ACKNOWLEDGMENTS

I thank J. M. Frost, K. T. Butler, F. Brivio, R. X. Yang, L. A. Burton, D. O. Scanlon, and C. H. Hendon who performed the original simulations discussed in this work, M. van Schilfgaarde for useful discussions on many-body physics, and L. M. Peter for insights into experimental aspects. I acknowledge funding from the Royal Society, the ERC (Grant 277757), and EPSRC Grants EP/J017361/1, EP/K016288/1, and EP/M009580/1.

## REFERENCES

- (1) Wyckoff, R. W. G. The Crystal Structures of Monomethyl Ammonium Chlorostannate and Chloroplatinate. *Am. J. Sci.* **1928**, *s5*–16, 349–359.
- (2) Weber, D.  $\text{CH}_3\text{NH}_3\text{SnBr}_{x-1}\text{I}_x$  ( $x=0-3$ ), a Sn(II)-System with the Cubic Perovskite Structure. *Z. Naturforsch.* **1978**, *33b*, 862–865.
- (3) Weber, D.  $\text{CH}_3\text{NH}_3\text{PbX}_3$ , a Pb(II)-System with Cubic Perovskite Structure. *Z. Naturforsch.* **1978**, *33b*, 1443–1445.
- (4) Poglitsch, A.; Weber, D. Dynamic Disorder in Methylammoniumtrihalogenoplumbates (II) Observed by Millimeter-wave Spectroscopy. *J. Chem. Phys.* **1987**, *87*, 6373–6378.
- (5) Onoda-Yamamuro, N.; Matsuo, T.; Suga, H. Calorimetric and IR Spectroscopic Studies of Phase Transitions in Methylammonium Trihalogenoplumbates. *J. Phys. Chem. Solids* **1990**, *51*, 1383–1395.
- (6) Wasylishen, R.; Knop, O.; Macdonald, J. Cation Rotation in Methylammonium Lead Halides. *Solid State Commun.* **1985**, *56*, 581–582.
- (7) Kojima, A.; Teshima, K.; Shirai, Y.; Miyasaka, T. Organometal Halide Perovskites as Visible-Light Sensitizers for Photovoltaic Cells. *J. Am. Chem. Soc.* **2009**, *131*, 6050–6051.
- (8) Bisquert, J. The Swift Surge of Perovskite Photovoltaics. *J. Phys. Chem. Lett.* **2013**, *4*, 2597–2598.
- (9) McGehee, M. D. Fast-Track Solar Cells. *Nature* **2013**, *501*, 323–325.
- (10) Snaith, H. J. Perovskites: The Emergence of a New Era for Low-Cost, High-Efficiency Solar Cells. *J. Phys. Chem. Lett.* **2013**, *4*, 3623–3630.
- (11) Kim, H.-S.; Im, S. H.; Park, N.-G. Organolead Halide Perovskite: New Horizons in Solar Cell Research. *J. Phys. Chem. C* **2014**, *118*, 5615–5625.
- (12) Jung, H. S.; Park, N.-G. Perovskite Solar Cells: From Materials to Devices. *Small* **2015**, *11*, 10–25.
- (13) Butler, K. T.; Frost, J. M.; Walsh, A. Ferroelectric Materials for Solar Energy Conversion: Photoferroics Revisited. *Energy Environ. Sci.* **2015**, DOI: 10.1039/C4EE03523B.
- (14) Egger, D. A.; Edri, E.; Cahen, D.; Hodes, G. Perovskite Solar Cells: Do We Know What We Do Not Know? *J. Phys. Chem. Lett.* **2015**, *6*, 279–282.
- (15) Brivio, F.; Walker, A. B.; Walsh, A. Structural and Electronic Properties of Hybrid Perovskites for High-efficiency Thin-film Photovoltaics from First-principles. *APL Mater.* **2013**, *1*, 042111.
- (16) Frost, J. M.; Butler, K. T.; Walsh, A. Molecular Ferroelectric Contributions to Anomalous Hysteresis in Hybrid Perovskite Solar Cells. *APL Mater.* **2014**, *2*, 081506.
- (17) Frost, J. M.; Butler, K. T.; Brivio, F.; Hendon, C. H.; van Schilfgaarde, M.; Walsh, A. Atomistic Origins of High-Performance in Hybrid Halide Perovskite Solar Cells. *Nano Lett.* **2014**, *14*, 2584–2590.
- (18) Butler, K. T.; Frost, J. M.; Walsh, A. Band Alignment of the Hybrid Halide Perovskites  $\text{CH}_3\text{NH}_3\text{PbCl}_3$ ,  $\text{CH}_3\text{NH}_3\text{PbBr}_3$  and  $\text{CH}_3\text{NH}_3\text{PbI}_3$ . *Mater. Horiz.* **2015**, DOI: 10.1039/C4MH00174E.
- (19) Brivio, F.; Butler, K. T.; Walsh, A.; van Schilfgaarde, M. Relativistic Quasiparticle Self-consistent Electronic Structure of Hybrid Halide Perovskite Photovoltaic Absorbers. *Phys. Rev. B* **2014**, *89*, 155204.
- (20) Hendon, C. H.; Yang, R. X.; Burton, L. A.; Walsh, A. Assessment of Polyanion ( $\text{BF}_4^-$  and  $\text{PF}_6^-$ ) Substitutions in Hybrid Halide Perovskites. *J. Mater. Chem. A* **2015**, DOI: 10.1039/C4TA05284F.
- (21) Walsh, A.; Scanlon, D. O.; Chen, S.; Gong, X. G.; Wei, S.-H. Self-Regulation Mechanism for Charged Point Defects in Hybrid Halide Perovskites. *Angew. Chem., Int. Ed.* **2015**, *54*, 1791–1794.
- (22) Yin, W.; Yang, J.; Kang, J.; Yan, Y.; Wei, S.-H. Halide Perovskite Materials for Solar Cells: A Theoretical Review. *J. Mater. Chem. A* **2015**, DOI: 10.1039/C4TA05033A.
- (23) Giorgi, G.; Yamashita, K. Organic-Inorganic Halide Perovskites: An Ambipolar Class of Materials with Enhanced Photovoltaic Performances. *J. Mater. Chem. A* **2015**, DOI: 10.1039/C4TA05046K.
- (24) De Angelis, F. Modeling Materials and Processes in Hybrid/Organic Photovoltaics: From Dye-Sensitized to Perovskite Solar Cells. *Acc. Chem. Res.* **2014**, *47*, 3349–3360.
- (25) Even, J.; Pedesseau, L.; Katan, C. Theoretical Insights into Multibandgap Hybrid Perovskites for Photovoltaic Applications. *SPIE Photonics Eur.* **2014**, 9140, 91400Y.
- (26) Catlow, C. R. A.; Sokol, A. A.; Walsh, A. Microscopic Origins of Electron and Hole Stability in ZnO. *Chem. Commun.* **2011**, *47*, 3386–3388.
- (27) Calabrese, J.; Jones, N.; Harlow, R.; Herron, N.; Thorn, D.; Wang, Y. Preparation and Characterization of Layered Lead Halide Compounds. *J. Am. Chem. Soc.* **1991**, *113*, 2328–2330.

- (28) Mitzi, D. B.; Wang, S.; Feild, C. A.; Chess, C. A.; Guloy, A. M. Conducting Layered Organic-inorganic Halides Containing 110-Oriented Perovskite Sheets. *Science* **1995**, *267*, 1473–1476.
- (29) Rao, C. N. R.; Cheetham, A. K.; Thirumurugan, A. Hybrid Inorganic-organic Materials: a New Family in Condensed Matter Physics. *J. Phys.: Condens. Matter* **2008**, *20*, 083202.
- (30) Catlow, C. R. A.; Stoneham, A. M. Ionicity in solids. *J. Phys. C: Solid State* **1983**, *16*, 4321–4338.
- (31) Jansen, M.; Wedig, U. A Piece of the Picture-Misunderstanding of Chemical Concepts. *Angew. Chem., Int. Ed.* **2008**, *47*, 10026–10029.
- (32) Brgoch, J.; Lehner, A. J.; Chabiny, M. L.; Seshadri, R. Ab Initio Calculations of Band Gaps and Absolute Band Positions of Polymorphs of RbPbI<sub>3</sub> and CsPbI<sub>3</sub>: Implications for Main-Group Halide Perovskite Photovoltaics. *J. Phys. Chem. C* **2014**, *118*, 27721–27727.
- (33) Scanlon, D. O.; Dunnill, C. W.; Buckeridge, J.; Shevlin, S. A.; Logsdail, A. J.; Woodley, S. M.; Catlow, C. R. A.; Powell, M. J.; Palgrave, R. G.; Parkin, I. P. Band Alignment of Rutile and Anatase TiO<sub>2</sub>. *Nat. Mater.* **2013**, *12*, 798–801.
- (34) Walsh, A.; Butler, K. T. Prediction of Electron Energies in Metal Oxides. *Acc. Chem. Res.* **2014**, *47*, 364–72.
- (35) Walsh, A.; Payne, D. J.; Egdel, R. G.; Watson, G. W. Stereochemistry of Post-transition Metal Oxides: Revision of the Classical Lone Pair Model. *Chem. Soc. Rev.* **2011**, *40*, 4455–4463.
- (36) Ramesh, R.; Spaldin, N. A. Multiferroics: Progress and Prospects in Thin Films. *Nat. Mater.* **2007**, *6*, 21–9.
- (37) Kutes, Y.; Ye, L.; Zhou, Y.; Pang, S.; Huey, B. D.; Padture, N. P. Direct Observation of Ferroelectric Domains in Solution-Processed CH<sub>3</sub>NH<sub>3</sub>PbI<sub>3</sub> Perovskite Thin Films. *J. Phys. Chem. Lett.* **2014**, *5*, 3335–3339.
- (38) Stroppa, A.; Di Sante, D.; Barone, P.; Bokdam, M.; Kresse, G.; Franchini, C.; Whangbo, M.-H.; Picozzi, S. Tunable Ferroelectric Polarization and Its Interplay with Spin-orbit Coupling in Tin Iodide Perovskites. *Nat. Commun.* **2014**, *5*, 5900.
- (39) Perdew, J.; Burke, K.; Ernzerhof, M. Generalized Gradient Approximation Made Simple. *Phys. Rev. Lett.* **1996**, *77*, 3865–3868.
- (40) Perdew, J. P.; Ruzsinszky, A.; Csonka, G. I.; Vydrov, O. A.; Scuseria, G. E.; Constantin, L. A.; Zhou, X.; Burke, K. Restoring the Density-Gradient Expansion for Exchange in Solids and Surfaces. *Phys. Rev. Lett.* **2008**, *100*, 136406–4.
- (41) Heyd, J.; Scuseria, G. Efficient Hybrid Density Functional Calculations in Solids: Assessment of the Heyd Scuseria Ernzerhof Screened Coulomb Hybrid Functional. *J. Chem. Phys.* **2004**, *121*, 1187.
- (42) Skelton, J. M.; Parker, S. C.; Togo, A.; Tanaka, I.; Walsh, A. Thermal Physics of the Lead Chalcogenides PbS, PbSe, and PbTe from First Principles. *Phys. Rev. B* **2014**, *89*, 205203.
- (43) Bardeen, J.; Shockley, W. Deformation Potentials and Mobilities in Non-Polar Crystals. *Phys. Rev.* **1950**, *549*, 72.
- (44) Yamada, Y.; Nakamura, T. Near-band-edge Optical Responses of Solution-processed Organic-inorganic Hybrid Perovskite CH<sub>3</sub>NH<sub>3</sub>PbI<sub>3</sub> on Mesoporous TiO<sub>2</sub> Electrodes. *Appl. Phys. Express* **2014**, *7*, 032302.
- (45) Fan, L.-Q.; Wu, J.-H. NH<sub>4</sub>PbI<sub>3</sub>. *Acta Crystallogr., Sect. E* **2007**, *63*, i189.
- (46) Wang, F.; Yu, H.; Xu, H.; Zhao, N. HPbI<sub>3</sub>: A New Precursor Compound for Highly Efficient Solution-Processed Perovskite Solar Cells. *Adv. Funct. Mater.* **2015**, DOI: 10.1002/adfm.201404007.
- (47) Kieslich, G.; Sun, S.; Cheetham, T. Solid-State Principles Applied to Organic-Inorganic Perovskites: New Tricks for an Old Dog. *Chem. Sci.* **2014**, *5*, 4712–4715.
- (48) Filip, M. R.; Eperon, G. E.; Snaith, H. J.; Giustino, F. Steric Engineering of Metal-halide Perovskites with Tunable Optical Band Gaps. *Nat. Commun.* **2014**, *5*, 5757.
- (49) Noel, N. K.; Stranks, S. D.; Abate, A.; Wehrenfennig, C.; Guarnera, S.; Haghighirad, A.; Sadhanala, A.; Eperon, G. E.; Pathak, S. K.; Johnston, M. B. Lead-Free Organic-Inorganic Tin Halide Perovskites for Photovoltaic Applications. *Energy Environ. Sci.* **2014**, *7*, 3061–3068.
- (50) Walsh, A.; Watson, G. W. Influence of the Anion on Lone Pair Formation in Sn(II) Monochalcogenides: A DFT Study. *J. Phys. Chem. B* **2005**, *109*, 18868–18875.
- (51) Eperon, G. E.; Stranks, S. D.; Menelaou, C.; Johnston, M. B.; Herz, L. M.; Snaith, H. J. Formamidinium Lead Trihalide: A Broadly Tunable Perovskite for Efficient Planar Heterojunction Solar Cells. *Energy Environ. Sci.* **2014**, *7*, 982–988.
- (52) Nagane, S.; Bansode, U.; Game, O.; Chhatre, S. Y.; Ogale, S. CH<sub>3</sub>NH<sub>3</sub>PbI<sub>(3-x)</sub>(BF<sub>4</sub>)<sub>x</sub>: Molecular Ion Substituted Hybrid Perovskite. *Chem. Commun.* **2014**, *50*, 9741–9744.